



**HAL**  
open science

## Solar shading and multi-zone thermal simulation: Parsimonious modelling at urban scale

Enora Garreau, Thomas Berthou, Bruno Duplessis, Vincent Partenay,  
Dominique Marchio

► **To cite this version:**

Enora Garreau, Thomas Berthou, Bruno Duplessis, Vincent Partenay, Dominique Marchio. Solar shading and multi-zone thermal simulation: Parsimonious modelling at urban scale. *Energy and Buildings*, 2021, 249, pp.111176. 10.1016/j.enbuild.2021.111176 . hal-03324083

**HAL Id: hal-03324083**

**<https://hal.science/hal-03324083>**

Submitted on 2 Aug 2023

**HAL** is a multi-disciplinary open access archive for the deposit and dissemination of scientific research documents, whether they are published or not. The documents may come from teaching and research institutions in France or abroad, or from public or private research centers.

L'archive ouverte pluridisciplinaire **HAL**, est destinée au dépôt et à la diffusion de documents scientifiques de niveau recherche, publiés ou non, émanant des établissements d'enseignement et de recherche français ou étrangers, des laboratoires publics ou privés.



Distributed under a Creative Commons Attribution - NonCommercial 4.0 International License



21 in most cases the most parsimonious choice for thermal heating demand simulation at district scale. Eventually, the  
22 coupling between thermal zoning models and solar shading models is analysed through the same methodology for  
23 assessing the modelling parsimony. The results show that the combination of simpler models (in particular a thermal  
24 zone per floor or mono-zone buildings for thermal zoning models, and a solar shading coefficient calculated per floor or  
25 facade for solar models) can be parsimonious enough to be used to determine the annual heating demand, speeding up  
26 strongly the simulation at the same time.

## 27 **Keyword**

28 Urban building energy simulation, thermal zoning design, solar shading calculation, parsimonious modelling

## 29 **1 Introduction**

30 The building sector is one of the most energy consuming sectors in the world, accounting for more than one third of the  
31 final energy consumption [1]. With the growing urbanization, approximately 68% of the world population will be  
32 residing in cities in 2050 [2]. In order to analyse and limit the impact of these trends, urban-scale building energy  
33 modelling (UBEM) tools are developed (DIMOSIM [3], SMART-E [4], City Energy Analyst [5], CitySIM [6],...).  
34 These UBEM can be used in very different contexts: the purposes of UBEM simulations can range from buildings  
35 retrofit potential ([7], [8]) to the sizing and control of thermal and/or electrical network ([9], [10]), to the calculation of  
36 renewable energy potential ([11], [12]) or to district multi energy system optimization ([13], [14]). It requires both a  
37 detailed level of building-scale modelling and a representation of the interactions that arise at district-scale. Moreover,  
38 the energy simulation at a district level leads to an increase of uncertainties. Collecting exhaustively building  
39 information data for parameterization is nearly impossible and the use of very detailed models becomes too expensive  
40 in computational time. The right models for each UBEM end-user must be identified to respond to these problems.

41 One of the urban simulation issues for the modeller is the thermal zoning design. The latter can create significant  
42 thermal variations as the solar gains are directly function of facade orientation, as the occupancy differs following the  
43 zone use (internal gains or HVAC set-points) or as the zones do not have the same external wall surfaces. Thermal  
44 division at district scale must a priori bring a better precision, but the models are difficult to set up with the lack of data  
45 and the simulation becomes rapidly too costly in computation time. As the simulation and set up times can be restrictive  
46 for urban simulation, the precision gain must justify the additional computation time. The multi-zone division of  
47 building is also related to the conductive and convective exchanges inside a building. Perez et al. [15] showed that

48 adiabatic walls in a multi-zone simulation can lead to more than 11% difference in thermal heating demand on one  
49 building. Nevertheless, further questions arise, in particular on the impact of the ventilation exchanges modelling, or on  
50 the sensibility of the multi-zone thermal modelling to solar gains calculation. For a mono-zone approach the solar gains  
51 are aggregated but for a multi-zone approach the solar gains are applied for each orientation and each altitude,  
52 influencing the HVAC systems. The modeller must then find and choose the solar gain models to keep the increase in  
53 accuracy from the thermal zoning models.

54 Indeed, the aim for the modeller is to find a trade-off between the availability and quality of inputs data and the level of  
55 detail of the models regarding the simulation's objectives, namely *a parsimonious modelling*. However, two opposite  
56 trends exist at urban scale: to develop more detailed urban models to gain in accuracy and to simplify more the models  
57 to accelerate the simulation. These developments are often done without knowing the relevance of such details  
58 regarding the simulation's objectives or the interaction with other models. Several studies have compared different  
59 modelling approaches but the conclusions are seldom generic since the analysis relies on specific districts or buildings.  
60 Frayssinet et al. ([16], [17]) compared different building sub-models as well as some interactions between buildings.  
61 The two most impactful models on the simulated district are the internal long wave model and the model taking the  
62 external convective heat transfer coefficients into account, with an underestimation of respectively 13 and 10 % on the  
63 mean heating power. The results are however not showing the interaction between the sub-models and are only applied  
64 on one district where the buildings show similar thermal characteristics. Han et al. [18] compared the inter-building  
65 effects (mutual shading and mutual reflection) at district scale on different cities in order to take the impact of climate  
66 into account. They showed a greater impact of the models on warmer climatic cities. Nevertheless, the study was  
67 applied on only one dense urban area. Robinson and Stone [19] developed a simplified solar radiation model, compared  
68 it to RADIANCE [20] (a reference tool for solar calculation) and validated it on a district. This simplification allows to  
69 reduce the computation time but can still be considered as a detailed algorithm for some simulation cases. Chen and  
70 Hong [21] compared 3 different zoning methods on 3 cities with results showing till 17 % difference in space heating  
71 load at district scale between two models. They advise to use one combination of models that balance precision and  
72 computation time, but do not propose to adapt it according to the district characteristics.

73 The diversity of models for each phenomenon at urban scale can be misleading for modellers and users, who have to  
74 choose the right adapted model and at the same time manage the time constraints and data accuracy. The multi-scale  
75 urban simulation implies various models for each phenomenon, which are linked to each other, and consequently

76 several interdependencies between families of models increasing the difficulty to select the complexity of multiple  
77 models.

78 The parsimony of a given model can be considered as the trade-off between the complexity and the accuracy of the  
79 model. This objective is presented in various studies ([22]–[24]), but most of them take the complexity only as the  
80 number of parameters, as the Aikake and Bayesian Information Criterion do ([25], [26]).

81 The paper proposes to investigate the influence of thermal zoning on energy demand of buildings at district scale, to  
82 couple it with the solar calculation models compared in [27], and to apply a parsimonious criterion. This criterion will  
83 allow to find the right combination of models that balance precision, time simulation and the amount of data required  
84 for parameterization, with the expected accuracy from the user. *The purpose is twofold: to analyse the impact of the  
85 simplified models and to find the different parsimonious combinations of models that respond to specific simulation  
86 objectives according to district characteristics. For the latter, the final objective is to guide UBEM users on the choice  
87 of models to use on real simulation cases.* Firstly, following the methodology framework proposed in [27], parsimony  
88 of multi-zone thermal modelling in buildings is investigated both at building scale and then at district scale. These  
89 zoning models are coupled with conductive and convective exchanges models to highlight the relevance of such model  
90 implementation, without direct shading: within this first step, the aim is to assess the impact of such models without any  
91 interference with shading models. Secondly, the coupling of a subset zoning/exchanges models and solar shading  
92 models is investigated. Finally, the study proposes perspectives of further work on the zoning division and more  
93 generally about the parsimonious modelling.

## 94 **2 Methodology**

95 *In most of UBEM, models are quite often adapted from building to district scale. They are separately tested on a  
96 specific district, but are seldom all compared on a variety of districts.* In order to make a parsimonious choice between  
97 these existing model adaptations, it is necessary to quantify the complexity of each model and their parsimonious  
98 nature. Therefore, a proposition for the analysis of modelling parsimony is presented, which relies on the definition of a  
99 parsimonious criterion and an inter-comparison process of models selected from the literature. Eventually, the results  
100 are analysed in regard to main districts characteristics in order to suggest key guidance indicators (KGI) for further  
101 decision-making processes.

## 102 2.1 Proposal for the analysis of modelling parsimony

### 103 2.1.1 Model complexity and parsimony quantification

104 For a specific model, a parsimonious criterion must be calculated to quantify its complexity in the most objective way.  
105 Modelling parsimony for urban energy simulation can be understood regarding numerous factors: the number of  
106 parameters, their complexity of recovery and their uncertainty, the model development time (and the time to parameter  
107 it), the accuracy of simulation, etc. Heidarinejad et al. [28] proposed a parsimonious approach for building sector that  
108 takes as complexity both computation and data recovery time. They applied it on a building simulation and compared it  
109 with the accuracy of their models. Here, we propose to quantify a parsimony criterion for urban scale simulation that  
110 takes into account multiple characteristics (Table 1). We considered four different entities related to urban simulation:  
111 parameters, time (computation or parametrization), models and simulation context. The latter was discarded for the  
112 creation of the criterion, as it is mostly linked to the KPIs (e.g.: the scale of the simulation is considered when choosing  
113 the KPI at building or district scale) and to simulation constraints (limit of computation time). The remaining  
114 parameters were combined to create several criteria that were tested on simple occupant models. A subset of these  
115 criteria was selected based on their results diversity and their ease of reading. Then, different weights were tested on  
116 their composition elements. In order to leave room for flexibility to the user, the criterion with coherent variation of  
117 results following the weights was selected. We propose then a parsimony criterion  $P_{\text{delta}}(M)$  for a model  $M$ , with  $N_M$   
118 parameters, that takes into account some of the characteristics of Table 1:

$$P_{\text{delta}}(M) = (a * AC + \text{Complexity}) - P_{\text{ref}} \quad \text{Eq. 1}$$

119 With AC the accuracy criterion (normalized root-mean square error, percentage error, etc.), and where:

$$\text{Complexity} = b * \sum_{i=0}^{N_M} w_i + c * H(M) \quad \text{Eq. 2}$$

$$P_{\text{ref}} = b * \sum_{i=0}^{N_{\text{ref}}} w_i \quad \text{Eq. 3}$$

120 With  $w_i$  the weights associated to the parameters of the model,  $H(M)$  the number of simplifying hypothesis and  $a$ ,  $b$ ,  $c$   
121 weight factors chosen by the user.  $w_i$  combine the complexity and the uncertainty related to data recovery and are  
122 determined thanks to a simple table (Table 2). This table was created with a combination of time recovery (based on  
123 Heidarinejad et al. [28]) and reliability (as proposed by the Cerema [29]).  $H(M)$  is evaluated against the reference: the  
124 aim is not to list every single simplifying hypothesis but to list the ones that enhanced the differences between the  
125 models. For example, if all thermal building models and their reference do not model the humidity, this assumption is

126 not accounted for. But if the reference is modelling it, then the models that do not consider the humidity must add a  
 127 simplifying hypothesis to H(M). The weight factors a, b and c are chosen by the user following his needs. For instance,  
 128 if other AC are chosen (not based on percentages but with other units), it is possible to adapt the factor a to have  
 129 comparable elements (number of hypothesis and parameters).

Parsimony topic	Topic characteristics	Determination
Parameters	Number of parameters	According to the models
	Data recovery complexity	According to the available databases
	Uncertainty	According to the enrichment tools <sup>†</sup>
Time	Model development time	According to the implementation complexity
	Model sizing time	According to the number of parameters and data recovery
	Computation time	According to the simulation type
Models	Accuracy	Accuracy measurement (NRMSE, PE,...) to choose
	Simplifying hypothesis	Number of neglected phenomena / simplifying hypothesis to represent the phenomena compared to the chosen reference
Simulation context		Description
Simulation scale		Spatial (zone, building, district) and temporal (min to year)
Study output		Establish the order of precision to obtain
Simulation type		Establish the order of limit simulation time following the type of simulation (sensitivity study, individual case...)

130 *Table 1: Characteristics of the urban-scale parsimony*

Weight $w_i$	Description
1	Reliable and easily accessible data (e.g.: public database) – Data recovery < 10-15 min
2	Reliable data but difficult to access (e.g.: cross-referencing of databases...) – Data recovery > 10-15 min
3	Unreliable data but no additional information available to corroborate them.
5	Data almost impossible to recover, so use default data.

131 *Table 2: Description of weights for data recovery and uncertainty*

132 The analysis is completed with the assessment of computation time. The latter is not used directly in the parsimony  
 133 criterion as it is too dependent of processing power or computer equipment. The AC is related to the KPI (for example  
 134 if a time series is studied, the normalized root-mean square or the Pearson coefficient can be used) and the researched  
 135 accuracy.

---

<sup>†</sup> Method/tool completing missing data

136 Some of the characteristics in Table 1 are put aside because they are already accounted for in other parameters: model  
137 sizing time is considered in the  $w_i$  as it is strongly related to data recovery time, and simulation scale is included in the  
138 AC. Model development time is not considered here as it is too difficult to quantify.

### 139 2.1.2 Modelling parsimony analysis

140 A comparative methodology is proposed in order to benchmark existing urban models. This process allows a  
141 comparison, *ceteris paribus*, of the models with each other. These models are taken from a representative sample  
142 selected from the literature and are compared to a common reference chosen from this sample. As validation data are  
143 indeed difficult to obtain at urban level, an inter-comparison approach appears as the most appropriate way for  
144 benchmarking. The selected models are, whenever possible, all implemented in one common simulation framework  
145 which removes any obstacles and biases linked to the comparison of models that are initially used with different  
146 simulation tools: in the present study DIMOSIM [3] has been used. These analyses are then performed following the  
147 methodology below (represented on Figure 1):

- 148 1) Selection of existing models and choice of a reference
- 149 2) Definition of KPI (Key Performance Indicator)

150 A KPI is quantifiable value directly calculated or derived (postprocess) from a model. Here two indicators are chosen:  
151 the thermal heating demand, assessed with the total percentage difference (PE), and the thermal heating load, assessed  
152 with the normalized root-mean square error (NRMSE). For a studied KPI  $Y = (y_0, y_1, \dots, y_n)$  and a model  $M$  :

$$PE(M, Y) = \frac{Y_M - Y_{ref}}{Y_{ref}} * 100 \quad Eq. 4$$

$$NRMSE(M, Y) = \sqrt{\frac{\sum_{i=1}^n (y_i - \hat{y}_i)^2}{n}} * \frac{1}{\bar{Y}} \quad Eq. 5$$

- 153 3) Selection of districts, whose characteristics are adapted to the context of the inter-model comparison.

154 The districts must present characteristics that are responsive enough to the studied phenomenon, so that the inter-model  
155 comparison makes sense. They are virtually created, based on existing morphologies (heights, densities and design are  
156 taken from GENIUS [30] results). They are selected with various characteristics to avoid realizing sensitivity analysis  
157 on parameters beforehand. The thermal parameters are created with data from the literature and French databases as  
158 well as projects TABULA [31] and PACTE [32].

- 159 4) Simulation of models at different temporal and spatial scales on a set of districts

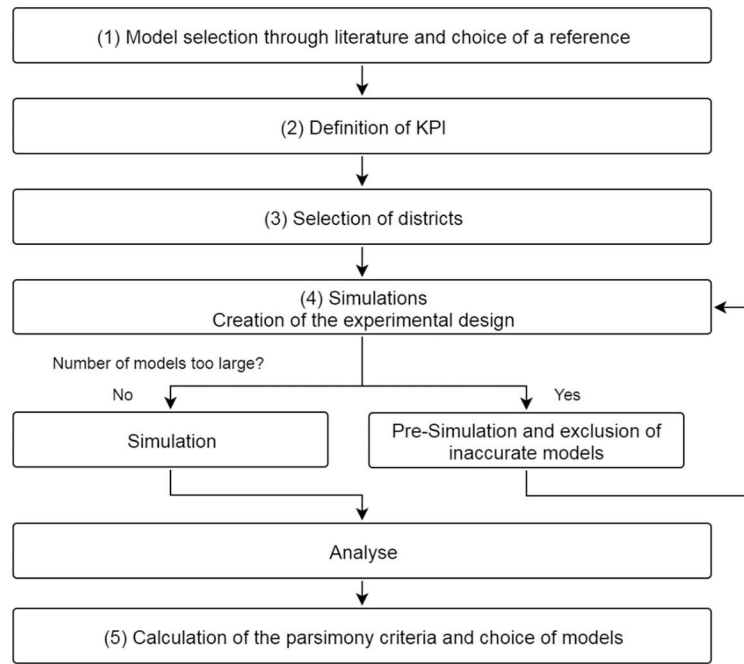
160 This inter-comparison is done by investigating the model combinations space with experimental designs. Here, the  
161 number of simulations for each single family being manageable, all the model and combinations (zoning with  
162 exchanges models) are used. When the combination of several model families imply to many simulations to launch, it is  
163 possible to do pre-simulations (either by using extreme districts, by using fractional factorial design (Saltelli et al. [33])  
164 or by selecting manually the combinations) to discard the too inaccurate models before simulating all the districts.  
165 When combining zoning and solar shading models, a manual selection is done to simulate only the relevant  
166 combinations at urban scale.

#### 167 5) Calculation of the parsimony criteria and selection of models

168 The parsimony criterion is applied on the KPI after determining the models characteristics. The results of the parsimony  
169 analysis are introduced through selection criteria (called Key Guidance Indicator, KGI) based on intrinsic properties of  
170 the districts (mean height, vegetation's area...). They help the modeller to choose, before any simulation, which type  
171 and level of detail of each model to use (see 2.1.3). Parsimony figures and tables are produced to ease the reading of  
172 results. The parsimony figure shows the parsimony criteria compared to the user's acceptable accuracy limit (called  
173 *limit error*) and the parsimony of the reference (at 0, see Eq. 1).

174 In the context of the present paper, the previously proposed approach is implemented three times to analyse the  
175 parsimony of zoning and shading modelling as well as their coupling. Firstly, the parsimonious analysis is carried out  
176 on single model family to avoid biased analysis through error compensation and to select the relevant parsimonious  
177 models for both families. Then, all the selected models are combined and analysed with the same parsimonious analysis  
178 frame. Therefore, the results sections of the present paper present the following developments:

- 179 1) Parsimony analysis of zoning models, combined with conductive and convective exchanges;
- 180 2) Parsimony analysis of shading models;
- 181 3) Parsimony analysis of the combination of the previously selected solar shading and zoning models.



182

183

Figure 1: Parsimony analysis proposal

184 2.1.3 Key indicators for analysis (KGI)

185 In order to analyse the outcomes of the inter-comparison process according to buildings and districts main  
 186 characteristics, building and district Key Guidance Indicators (KGI) are created. These analysis parameters have been  
 187 named “Key Guidance Indicators” in order to be used *in fine* as selection parameters of a parsimonious modelling  
 188 approach by the users of UBEM tools.

189 These indicators are designed on parameters that must remain global enough to be available at district scale. At building  
 190 scale, geometry parameters (e.g.: height, ground surface), usage parameters (e.g.: internal gains, usage type), but also  
 191 thermal parameters (e.g.: U-values, window-to-wall ratio) are relevant candidates. At the district scale the mean and the  
 192 standard deviation of those parameters can be used to reflect the diversity of some parameters among buildings in a  
 193 district. In the present paper, parameters composing the KGI have been chosen by using Spearman coefficient to detect  
 194 the most correlated ones with the differences between models. This coefficient is a non-parametrical measurement of  
 195 statistical dependency between two variables. It indicates if a monotonic dependency exists, without being necessarily  
 196 linear, with a formula on the ranks:

$$r_{spearman}(X, Y) = \frac{cov(rang_X, rang_Y)}{\sigma_{rang_X} \cdot \sigma_{rang_Y}} \quad Eq. 6$$

197 These parameters are combined, tested and adapted to the simulation results to elaborate the best KGI to help the  
198 modeller choose which model is the most parsimonious before any simulation. This last step is done mostly with  
199 “expert knowledge” to choose the KGI allowing the least result diffusion and the best readability.

## 200 **2.2 Thermal zoning and demand modelling of buildings**

201 At building scale numerous studies were undertaken on the thermal zoning of building ([15], [34]–[37]). The multi-  
202 zone approach takes into account the disparities in building, whereas the mono-zone modelling blends the internal and  
203 solar gains. To compensate a possible lack of accurate data, some tools propose to divide automatically the buildings  
204 into perimeter and core zones, for example Autodesk [38] from the ASHRAE recommendation. However, the methods  
205 are neither adequately described nor open source. Smith [37] compared 7 zoning configurations (one with one zone per  
206 floor, the other with core/perimeter zones per floor with different depth and zone length) on 3 building geometries, to  
207 the ASHRAE recommendations. The differences to the reference went till 40 % for fuel consumption, but only 10 % for  
208 electricity consumption. Martin et al. [34] compared several zoning models (mono-zone, one zone per floor and  
209 perimeter/core zones per floor) on an office building with EnergyPlus. If simpler models helped reduce the computation  
210 time, they also increased the error (1 to 13 %) in cooling consumption. Shin et al. [39] showed through a literature  
211 review that today no precise thermal zoning rules exist but only simple guidance principles and parameters to take into  
212 account.

213 If at the building scale it is already difficult to propose general guidance principles, it is even more complicated at urban  
214 scale. Few studies are applied at this scale. Chen and Hong [21] compared different thermal zoning on three different  
215 climatic cities, showing till 80% differences at building scale and 20% at district scale for annual source energy use.  
216 They compared a one zone per floor zoning, a core/perimeter per floor zoning method based on the AHRAE  
217 recommendations, and a prototype method which use prototypes buildings with given zoning models. In this method,  
218 offices are divided with 4 perimeter zones, 1 core zone and 1 plenum zone. Dogan et al. ([40], [41]) developed an  
219 algorithm to automatically divide every floor of a building into core and perimeter zones (one per orientation). They  
220 coupled it with a simplifying simulator to only simulate a set of zones for entire buildings, and therefore achieved to  
221 reduce computation time for entire districts. When looking at UBEM tools, some of them allow the modelling of  
222 buildings in a detailed manner, but thermal zoning is simplified when simulating an entire district because of  
223 computation time cost and lack of data. Because of it, only general zoning methods following the type of building usage  
224 can be used on entire districts. This geometry zoning is part of the building thermal model that influences the energy

225 results. This study proposes then to investigate the impact of several zoning layouts on residential and office buildings  
226 only.

227 However, the thermal zoning issue cannot be separated from the question of thermal exchanges between zones. These  
228 thermal exchanges are composed of conductive exchanges through walls or convective ones with air movement  
229 (buoyancy or mechanical ventilation). With a mono-zone building these phenomena cannot be modelled, but as soon as  
230 multiple zones are created the exchanges can be impacting, especially when the zones are divided by orientation. The  
231 exchanges allow to mitigate the gains through the building and to account for the impact of multiple uses with different  
232 temperature or gain profiles. Therefore, this study investigates the coupling between several geometry modelling with  
233 thermal exchanges models.

#### 234 *2.2.1 Thermal and heat transfer models*

235 In the present study, simulations are done on the UBEM DIMOSIM [3] developed by CSTB. DIMOSIM is an  
236 integrated simulation tool for the analysis of feasibility, conception and operation of district energy systems. Based on  
237 building and thermal zone models DIMOSIM can deal with various energy systems at building (generators, emitters,  
238 hydronic distribution, storage, etc.) and district scale (thermal and electricity networks).

239 The thermal model in DIMOSIM is a simplified physical model from the grey RC model family. The model is a  $R_iC_j$   
240 model that can adapt himself on the input data. The model is briefly described in [42]. Two variants developed in  
241 DIMOSIM are to be tested:

- 242 - Ex0: The exchanges through walls or floors are neglected between zones (adiabatic walls) and only the  
243 thermal inertia is considered.
- 244 - Ex1: The exchanges between adjacent zones are taken into account thanks to a R2C3 model for each wall. We  
245 suppose the wall symmetrical and with the same composition.

246 [For each zoning configuration the building total thermal mass is the same.](#)

#### 247 *2.2.2 Ventilation models*

248 In a building there are several air exchanges: infiltration, mechanical ventilation and buoyancy ventilation (through  
249 doors and interstices). At building scale, it is possible to model them from pressure calculation or fluxes balance. For  
250 example, TRNSYS and EnergyPlus propose several methods of calculation with nodal models in order to couple  
251 thermal and aeraulic modelling. More detailed models simulate the effect of the wind on walls to evaluate air flows

252 entering the building, as the Envi-MET [43] or Design Builder [44]. In this study only the inside air flows are studied,  
253 we suppose that the outside air flows are constant and not interacting with the ventilation.

254 The multi-zone ventilation models can be solved simultaneously with the thermal model, with a pressure balance which  
255 requires the knowledge of very detailed parameters such as the window position or the size of the interstices. For the  
256 urban ventilation we consider here that the recovery of all these data is too difficult to obtain and that this type of  
257 simulation would be intrinsically un-parsimonious. A simple ventilation is then proposed for residential and office  
258 buildings to still take the exchanges into account but only with air flows on floors, with no vertical connections:

- 259 - V0: A common air change rate scenario is applied for infiltration and ventilation and the ventilation losses are  
260 calculated from a simple ventilation system or a ventilation system with heat recovery:

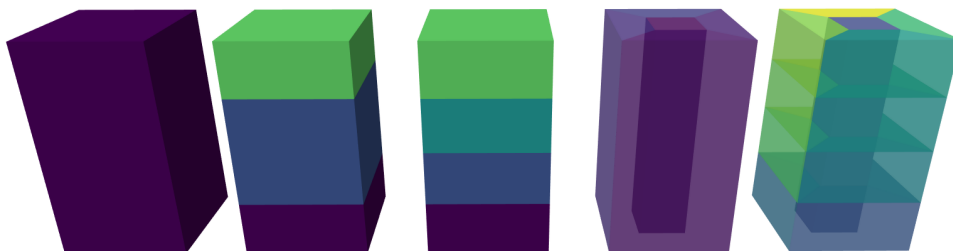
$$Q_{ventilation,losses} = \dot{m} * c_{p_{air}} * (1 - \varepsilon) * (T_{ext} - T_{air}) \quad Eq. 7$$

261 *With  $\dot{m}$  the air flow rate,  $\varepsilon$  the ventilation efficiency and  $T$  the outdoor and thermal zone air temperatures*

- 262 - V1h: Ventilation for residential buildings. Central zones are often common spaces for circulation, and  
263 ventilation is managed per dwelling. Nevertheless, air exchanges happen naturally by buoyancy between the  
264 perimeter zones (the dwellings) and the core zone (corridor). This type of ventilation is modelled with the  
265 correlation from Caciolo [45] as a single-faced natural ventilation for each door.
- 266 - V1b: Ventilation for office buildings. Ventilation of central areas plays an important role as they are often  
267 subject to overheating. Therefore, an air exchange is added to V1h: the air flows from the perimeter to the core  
268 zone on a single floor thanks to the mechanical ventilation.

### 269 2.2.3 Thermal zoning models

270 From the literature five models were chosen and implemented in DIMOSIM. As the computation time depends on the  
271 number of zones and surfaces, the chosen models must cover a wide range of zoning division, from the simplest one, to  
272 a detailed one used for urban simulation. Two groups of models are taken into account: the floor models (based on the  
273 idea of one zone per floor) and detailed models (based on orientation) (Figure 2).



274

275 *Figure 2: The zoning geometries on a building – from left to right: unique, 3 floors, multiple floors, detailed, detailed floor*

## 276 **Floor geometries**

277 Three different geometry with vertical zoning are proposed

- 278 - *Unique*: The mono-zone building with only one zone per building. It is mostly used in urban simulation  
279 because of the computation time and the basic information on geometry.
- 280 - *3 floors*: A simplified floor model is implemented. As for Chen and Hong [21], only three zones are created in  
281 the building: the top floor, the bottom floor and a unique zone with all other floors in between. It allows to  
282 speed up the simulation for very tall buildings by assuming that all middle floors have the same occupation,  
283 usage and systems.
- 284 - *Multiple floors*: One zone is created per floor with a floor height taken as 3 m. It is assumed that no uncertainty  
285 is present for the mean floor height. It is then possible to differentiate the usages per floor and to take different  
286 solar radiation per height if the solar masks are taken into account.

## 287 **Detailed geometries**

288 Two different horizontal geometries based on orientation are implemented:

- 289 - *Detailed*: The division is done to have a thermal zone per wall orientation around a central zone. *An area is*  
290 *created within the convex polygon to represent the central zone and perimeter zones are created around it, one*  
291 *per wall segment*. If the building footprint is too small, no central zone is created and the perimeter zones are  
292 determined from the centroid of the polygon. The perimeter zones are 5 m or 3 m deep, according to the size of  
293 the building. For concave building, the zone division can lead to too narrow or twisted zones like presented by  
294 Dogan et al. [40]. As the study uses virtual buildings, a central line is implemented also virtually to help create  
295 more realistic zones.
- 296 - *Detailed floor*: This model is the combination of the *multiple floors* and the *detailed* model. All the central  
297 zones per floor are combined in one to accelerate the simulation and to keep modelling consistency: it is  
298 assumed that all the central zones are connected to each other through stairs or lifts with the same usage and  
299 gains.

### 300 *2.2.4 Buildings characteristics and occupation*

301 Thermal parameters are taken from TABULA and PACTE (U-value of the walls, roofs, floors and windows, the  
302 window transmission factor, the window share and the infiltration rate) and are randomly attributed to a building

303 geometry (created from uniform distribution on the height, the orientation and the ground floor size). The European  
304 project TABULA analysed the residential building stock of several countries, and for each created typologies (40 for  
305 France) by classifying them following architecture and energetic parameters. Different levels of renovation are  
306 proposed for each typology. The French PACTE program aimed also to analyse the French building stock thanks to  
307 existing studies and data in order to obtain a classification of residential buildings in the light of national energetic  
308 objectives. The information of both databases have been cross-referenced and linked together to get more accurate  
309 building distribution and characteristics. The objective is to have representative buildings of French building stock for  
310 the simulations, with the right representativeness by weighting each typology to their existing proportion in the stock  
311 when creating the building sample. To introduce more diversity, a sizing factor for internal gain is applied for each  
312 building profile to modify their order of magnitude.

313 When dividing a building per zone, it is possible to consider different uses and occupation profiles. In this study, two  
314 occupancy scenarii are presented for the analysis:

- 315 - *Same*: all thermal zones have the same internal gains, set-point temperatures and usages.
- 316 - *Centre*: Central zones for the detailed zoning have different scenarii, with no heating and cooling. For  
317 residential building the central internal gains (W/m<sup>2</sup>) are reduced to 10% of their initial value. For the office  
318 they are reduced to 80% of their initial value, as the meeting rooms and informatics centres are considered  
319 there. For the floor geometries, it is considered that the user doesn't take this central zone into account when  
320 applying the gains and temperatures. The simulations are then the same with the scenario *same* or *centre*.

321 Other occupation scenarii were studied but are not presented, as zones vacancy in residential buildings, internal gains  
322 and temperature variation between zones within one building, or usage variation with tertiary occupancy at the bottom  
323 floors.

324 Here only full residential and full office buildings are considered, with custom profiles for each usage (see Figure 3)  
325 through the week. Heating (September to May) and cooling (June to end of August) seasons are implemented.

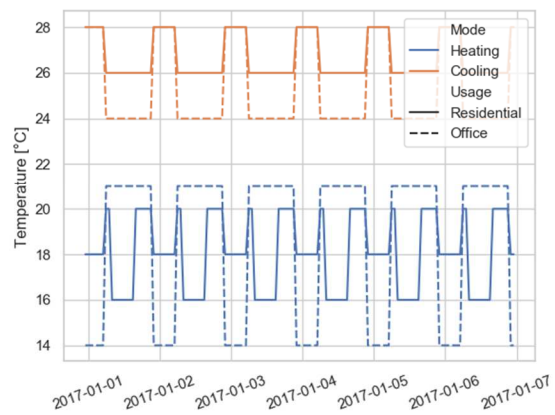
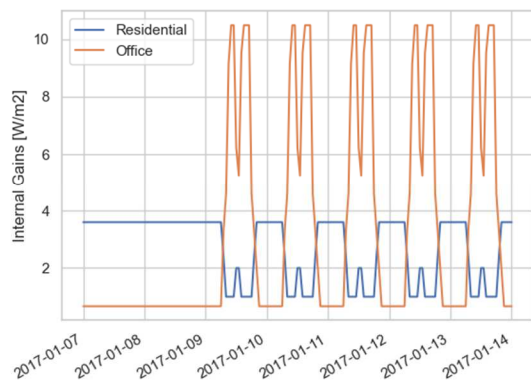


Figure 3: Internal gains (left) and set-point temperatures (right) for one week for residential and office buildings

326  
327

328 Other occupancy profiles could be added with different thermal zoning design following the usages of buildings. For  
 329 example, Chen and Hong [21] adapted the zoning design for retail usages to take into account storage zones.  
 330 In the simulations, all buildings are in a rectangular shape, with ideal building generators and ideal control. For the  
 331 parsimony analysis of thermal zoning modelling, no shading mask is calculated.

### 332 2.2.5 Computation implementation

333 Simulations are run on a computer server, which can run up to 64 simulations simultaneously (64 cores). Simulations  
 334 are done over one year with a time step of 10 min. For the office building simulations, the time step is reduced to 5 min  
 335 because of convergence constraints due to the ventilation model. The Paris Montsouris weather (TMY2-71560) is used.

## 336 3 Comparative assessment of solar shading and thermal models without coupling

### 337 3.1 Results for thermal zoning models

338 The models being focused on the building itself and not intrinsically on the district, it is necessary to first analyse the  
 339 results at building scale: it allows to detect the most influential families (zoning, thermal exchange, ventilation  
 340 exchanges) and discard the too inaccurate models. Then, an analysis can be undertaken on the remaining models to find  
 341 both the right KGI and the most parsimonious combinations of models at district scale. At the same time, it will be  
 342 possible to assess whether the diversity at district scale can reduce errors.

343 The modelling reference is taken as the combination of the most detailed models for each type of model: *detailed floor*  
 344 with conductive (Ex1) and convective exchanges (V1).

345 3.1.1 Computation time

346 Table 3 presents the computation time for two buildings of different heights with a floor height of 3 meters. The first  
 347 building is 6 m high (equivalent to 9 thermal zones for the *detailed floor* zoning), while the second is 21 m high  
 348 (equivalent to 29 thermal zones). The use of a ventilation model does not have much impact on the computation time,  
 349 with only a speed-up factor of 1.1. The conductive exchange model has a significant impact on the computation time  
 350 when the building is higher, with almost 40 s difference for the *detailed floor* zoning. But eventually, it is the zoning  
 351 models that affect the most the computation time: the simpler models accelerate the simulation, with speeding-factors  
 352 from 5 to 29. The higher the building, the greater the impact of simpler models on the computation time.

353 Table 3: Simulation time for two buildings (V0: without convective exchanges, V1: with convective exchanges)

Models	H = 6m		H = 21m	
	t [s]	Speeding factor	t [s]	Speeding factor
<b>With conductive exchanges (Ex1)</b>				
Detailed floor – V1	29	1	123	1
Detailed floor – V0	28	1	116	1.1
Detailed – V1	17	1.7	18	6.9
Detailed – V0	16	1.7	17	7.4
Multiple floors	8	3.7	24	5.1
3 floors	8	3.5	11	11.5
<b>Without conductive exchanges (Ex0)</b>				
Detailed floor – V1	26	1.1	81	1.5
Detailed floor – V0	26	1.1	69	1.8
Detailed – V1	16	1.8	15	8.4
Detailed – V0	15	1.9	14	9
Multiple floors	7	4	18	6.7
3 floors	7	4	9	14.1
Unique	4	6.5	4	29.3

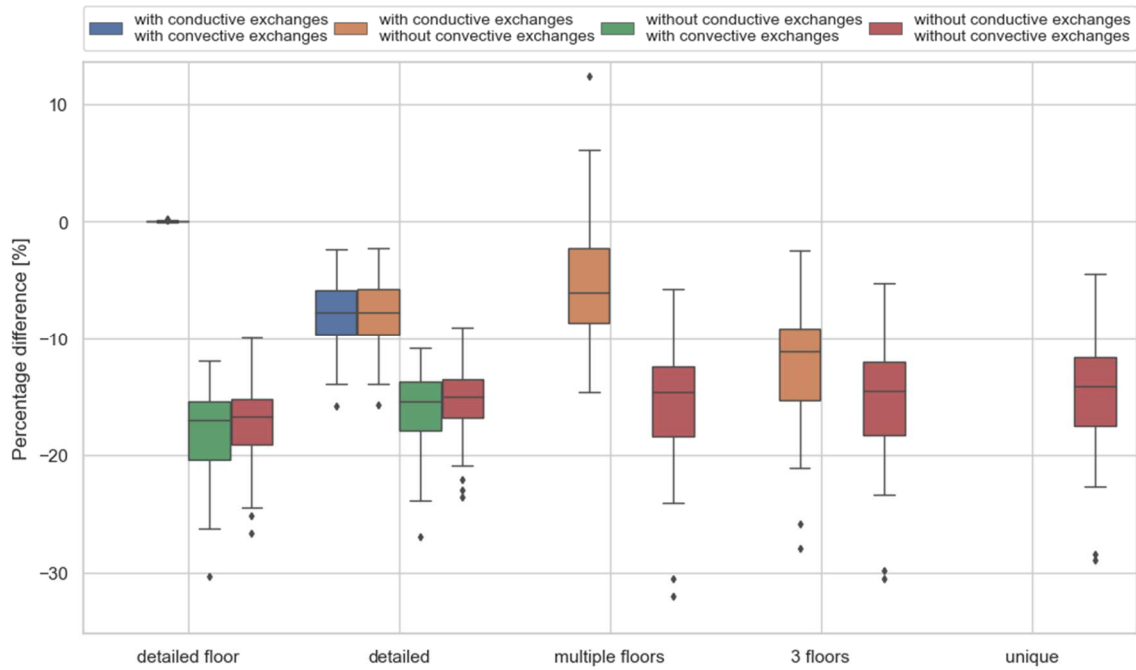
354 3.1.2 Heating demand simulation at building scale

355 A first comparison of the influence of thermal zoning models at building scale on heating demand simulation is  
 356 presented. By comparing the buildings results to the reference, it is possible to visualize the errors (Figure 4) in order to  
 357 quickly discard the unsuitable models and to understand the discrepancies.

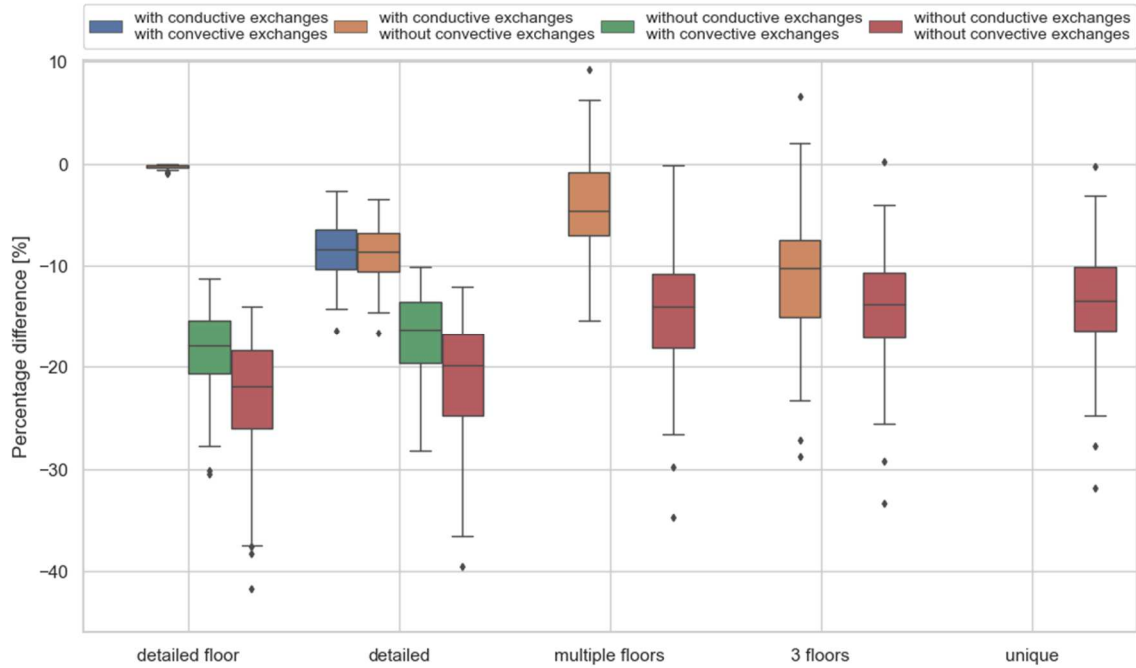
358 Following the scenario, the models have different results. For the *same* scenario, ventilation exchanges do not have a  
 359 significant influence on the detailed models. On the other hand, the use of this model for the *centre* scenario reduces the  
 360 differences when no conductive exchanges are modelled (around 10%). Ventilation with the central zone tempers  
 361 actually the temperatures of the perimeter ones. The differences for the floor division models are smaller for the *same*  
 362 scenario because of the homogeneity of the internal gains and temperatures on one floor. However, except for the

363 ventilation's impact, the relative differences between models for both occupancy scenarii are quite similar, with higher  
 364 errors for the *center* scenario. For the rest of the study, only the *center* scenario is analysed.

365 Both *detailed floor* and *detailed* models without any conductive exchanges present the worst results compared to the  
 366 reference. Therefore, if the zones are "orientation" divided, it becomes mandatory to take into account thermal  
 367 exchanges between thermal zones in order to achieve acceptable results.



368



369

370 *Figure 4: Annual thermal heating demand differences (PE) for residential buildings - Scenarii: up same - down center*

371 The *multiple floors* model presents good accordance with the reference, as most errors are approximatively within  $\pm 10$   
372 % when the thermal exchanges models are used. If they are not, the model presents almost the same results as the *3*  
373 *floors* model. These results are in agreement with the conclusions of Martin et al. [34], who found out that the multi-  
374 floor models give better estimates of cooling demand than other simple models. When buildings are wider, the  
375 influence of the central zone increases compared to the perimeter zones, until a balance is reached where the global  
376 heating demand is the same as a simple floor zone. The *unique* model has discrepancies in the same range as the other  
377 floor models (between -5 and -30 %), with a significant difference in time. These differences are similar than the ones  
378 from other thermal zoning comparisons on heating demand in the literature, as for example Perez et al. [15] who found  
379 -18 % error between a detailed division and a unique zone, or Heo et al. [36] who calculated an error of -24 % between  
380 a 11-zone model and a mono-zone building. Almost all of the floor division models underestimate the heating demand  
381 due to the counterbalance of the orientation by the floor aggregation: the core and perimeter zones cancel out each other  
382 heating demand. This underestimation in thermal demand for zoning that do not consider orientation was also found by  
383 Smith [37].

384 From these results, and by choosing a maximal acceptable error of 10% in heating demand, only the detailed models  
385 without any conductive exchanges are put aside. The most accurate ones are the *detailed floor*, *multiple floors*, *detailed*  
386 with conductive exchanges (with or without ventilation exchanges). However, the floor models show errors between  
387  $\pm 10$  % for some buildings and present at the same time low computational times (4 to 30 times faster). They are then  
388 kept for the district aggregation. In the following text, the conductive exchanges models are name EX, and the  
389 convective V.

390 The NRMSE on the heating loads was also studied (not shown here): the relative difference between models are the  
391 same, with a median NRMSE between 3 % (*detailed floor* with exchange and without ventilation) and 36 % (*detailed*  
392 *floor* without exchange and ventilation). For the latter model, the NRMSE reaches a maximum of 57 %. The same  
393 conclusions on the choice of models are reached.

394 The same analysis was also done with office buildings, where only the internal gains and temperatures profiles  
395 parameters are modified. It shows similar results than for the residential buildings with higher differences, especially  
396 for the NRMSE with a median for office buildings between 5 and 47 % (maximum of 110 %).

### 397 3.1.3 Heating demand simulation at district scale

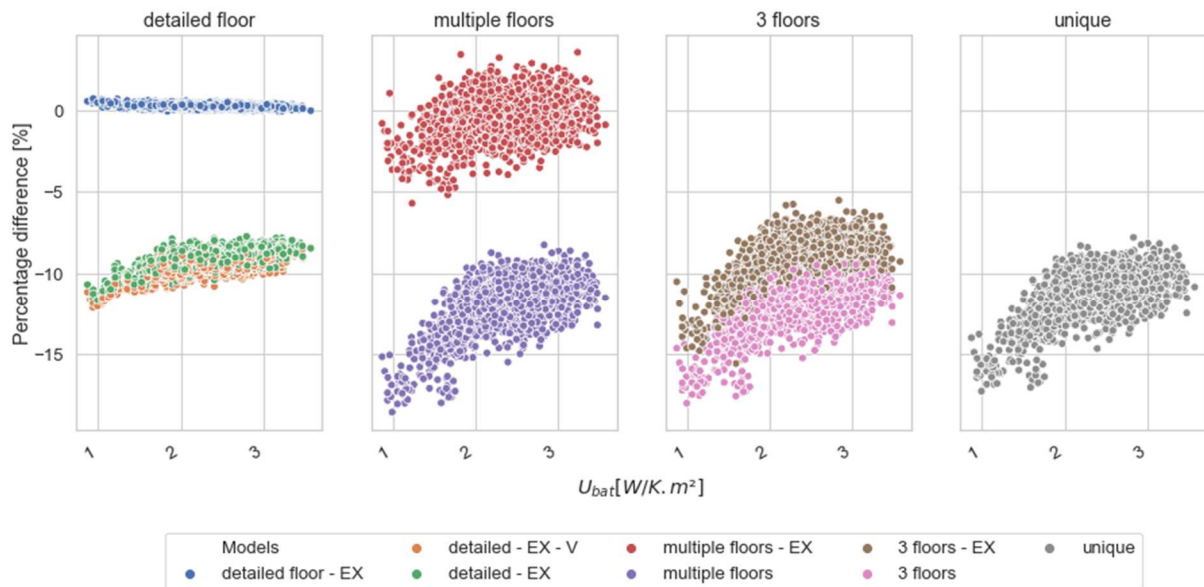
398 At a district scale there is a diversity of buildings, allowing error compensation. Given the previous results, some  
399 models should have the same impact than at building scale regarding the constant difference to the reference. Others

400 have differences that should mitigate the global discrepancies at district scale. To highlight these spatial differences,  
 401 2000 districts of 50 buildings are randomly created with the *centre* scenario (buildings with residential or office uses).  
 402 The heating demand is simply taken as the sum of all building heating demands.

403 Figure 5 presents the variation of error as a function of the mean  $U_{bat}$  of the district (weighted by the ground floor area  
 404 of each building). This parameter is taken for each building as the mean U-value of the opaque and window U-values  
 405 weighted by the surfaces:

$$U_{bat} = \frac{\sum U_{opaque} * S_{opaque} + U_{window} * S_{window}}{S_{total}} [W/m^2.K] \quad Eq. 8$$

406 As expected, the model *multiple floors* - EX shows good agreement with the reference thanks to the diversity of  
 407 buildings. This is in concordance with the simulations of Chen and Hong [21] at district scale without any thermal  
 408 exchanges. Indeed, they advised the use of a multi-floor design for thermal demand simulation, as well as an adapted 3-  
 409 floors model to speed up the simulations for high-rise buildings. Without exchanges, the *multiple floors* and *3 floors* are  
 410 indeed in the same range of errors: the *3 floors* model could be used to accelerate the simulation for high-rise buildings  
 411 (Table 3).



412

413 *Figure 5: Percentage difference of the district annual heating demand following the mean  $U_{bat}$  of the district*

414 According to the mean  $U_{bat}$  of the district, it is possible to identify trends: the more the district incorporates new  
 415 generation buildings, the more the detailed zoning models are useful. Indeed, in old buildings the thermal losses reduce  
 416 the overheating in southern parts and mitigate temperatures differences: deviations of floor zoning models are then  
 417 reduced.

418 In order to have a less diffuse set of results for determining the switching values between the use of different models,  
 419 the sensitivity of errors to various parameters is studied. For each model and KGI-parameters, the Spearman coefficient  
 420 is calculated on the percentage difference to the reference. Only the parameters with an absolute value higher than 0.5  
 421 are kept. Then, to have only parameters with different impacts on the errors, a Pearson coefficient matrix is calculated  
 422 and only several parameters are kept:

- 423 - The  $U_{bat}$  [W/m<sup>2</sup>.K] (see Eq. 8)
- 424 - The compactness [m<sup>-1</sup>]: all building envelope surfaces divided by its volume;

$$Compactness = \frac{S_{external}}{V_{building}} [m^{-1}] \quad Eq. 9$$

- 425 - The infiltrations rate [h<sup>-1</sup>]
- 426 - The ground floor area  $A_{ground\ floor}$  [m<sup>2</sup>]

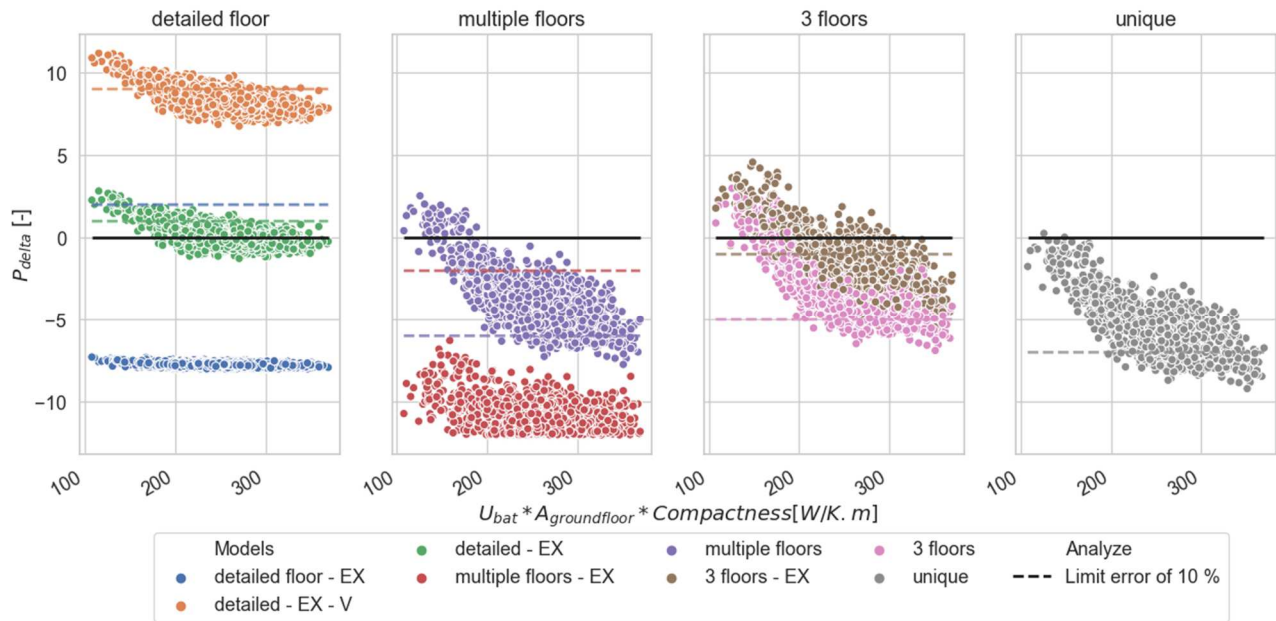
427 At district scale the mean value of each parameter weighted by the ground floor area of building is used (except for the  
 428  $A_{ground\ floor}$ ).

429 Various combinations of these parameters are done, until the identification of a KGI (called  $UAC$ ) composed of the  $U_{bat}$ ,  
 430 the ground floor area and the compactness:

$$UAC = U_{bat} * A_{ground\ floor} * Compactness [W/m.K] \quad Eq. 10$$

431 On Figure 6, the parsimony criterion  $P_{delta}$  (see Eq. 1) is applied on the previous results. The weight factors a, b and c are  
 432 taken as 1 (we consider here all parsimony elements of equal importance). The considered parameters for thermal  
 433 zoning models are building geometry, building usages, interior zones repartition and floor height. Conductive exchange  
 434 model parameters differ only by the consideration of the inner walls composition. As for convective exchanges models,  
 435 air change rate, ventilation type and opening areas for ventilation are considered. Each parameter is linked to a  $w_i$  value  
 436 (adapted for the French context) and to one or several models. The simplifying hypothesis are based on the type of  
 437 building zoning and the consideration of conductive and/or convective exchanges.

438 We consider that the inaccuracy of the models must not exceed 10 % for the heating demand. Therefore, a *limit error of*  
 439 *10 %* for each model (AC is taken as 10 % in  $P_{delta}$  to have the right criterion considering the complexity) is plotted  
 440 (dotted line) to eliminate easily the too inaccurate models. The parsimony of the reference is the line 0 (solid line): if  
 441  $P_{delta}$  is under this value the model is considered as parsimonious.



442

443

Figure 6: Parsimony criterion of district annual heating demand following the KGI UAC – Zoning models

444

445

446

447

448

449

450

451

452

453

454

455

456

457

458

459

460

When taking into account models complexity, *detailed* models have high criteria value: mostly above the parsimony of the reference (0) and partly above the acceptable error (dotted line). On the other hand, floor models without conductive exchanges have mostly criteria below 0, but still above the acceptable error. However, for high UAC values, i.e. mostly leaky buildings, the criterion  $P_{\text{delta}}$  has good values. Given the gain in terms of computation time, floor models become even more interesting than the *detailed floor* – EX, and could be chosen as part of the most parsimonious models. Nevertheless, the most parsimonious model whatever the UAC remains the *multiple floors* – EX. Only the *unique* model achieves equivalent criteria for high UAC.

The previous figure (Figure 6) highlights the spread of results. However, to help UBEM users, a simplified table is created expressing the previous results (Table 4) as follows:

- “Dark green” is the most parsimonious model, according to  $P_{\text{delta}}$  value: it is under the reference parsimony (0-value) and the acceptable error (here 10 %).
- “Light green” models are the recommended ones: they are parsimonious (under the 0-value) and with acceptable errors (here less than 10 %).
- “Yellow” models are possible to use: they are below the acceptable error (here 10 %) but they are not parsimonious (above the 0-value).
- “Red” models are to be avoided: they are neither parsimonious nor accurate enough (at least above the acceptable error, and at worst above the acceptable error and 0-value).

461 If the colour is shaded with another colour, models can be used either as the background colour or as the shaded colour:  
 462 results are too spread to determine one category in these cases. The choice of model must be then cautious. This table  
 463 can be combined with computation time to help choose the right model for a given simulation.

464 *Table 4: Models to prioritize for a district energy simulation following the UAC for annual heating demand – Zoning models (EX :*  
 465 *with conductive exchanges, V: with convective exchanges)*

Models	UAC [W/K.m]				
	150 <	200	250	< 320	
Reference	Green	Green	Green	Green	Green
Detailed floor – EX	Green	Green	Green	Green	Green
Detailed – EX - V	Red	Red	Orange hatched	Yellow	Yellow
Detailed – EX	Red	Orange hatched	Orange hatched	Green hatched	Green hatched
Multiple floors – EX	Green	Green	Green	Green	Green
3 floors – EX	Red	Red	Red	Brown hatched	Green
Multiple floors	Red	Red	Red	Red	Red
3 floors	Red	Red	Red	Red	Red
Unique	Red	Red	Red	Brown hatched	Green

466 A specific study was undertaken on the influence of climate on districts by using weathers from Strasbourg (continental  
 467 climate) and Nice (hot climate). The results are not shown here, but as for Chen and Hong [21], the impact of such  
 468 change in weather on heating demand has been calculated to be greater in warmer climates. These larger differences  
 469 limit the number of parsimonious models available.

#### 470 3.1.4 Conclusion and selection of models

471 In conclusion, for a district with mono-usage buildings (office or residential) under Paris weather, the zoning division  
 472 per orientation without considering floors is mostly inaccurate and not parsimonious enough. The division per floor  
 473 with conductive exchanges is however a good compromise between accuracy and complexity: it is a parsimonious  
 474 choice for urban simulation. To speed up the simulation it is possible to choose between other parsimonious models for  
 475 specific districts as *3 floors – EX* and *unique*.

476 With these parsimony results, a selection of models is done for coupling purposes. The floor models *multiple floors –*  
 477 *EX*, *3 floors – EX* and *unique* are kept as they present parsimonious results and low computation times. The *detailed –*  
 478 *EX* is preferred to *detailed – EX – V* as it presents better results. The reference and *detailed floor – EX* are also  
 479 selected. The other models are discarded.

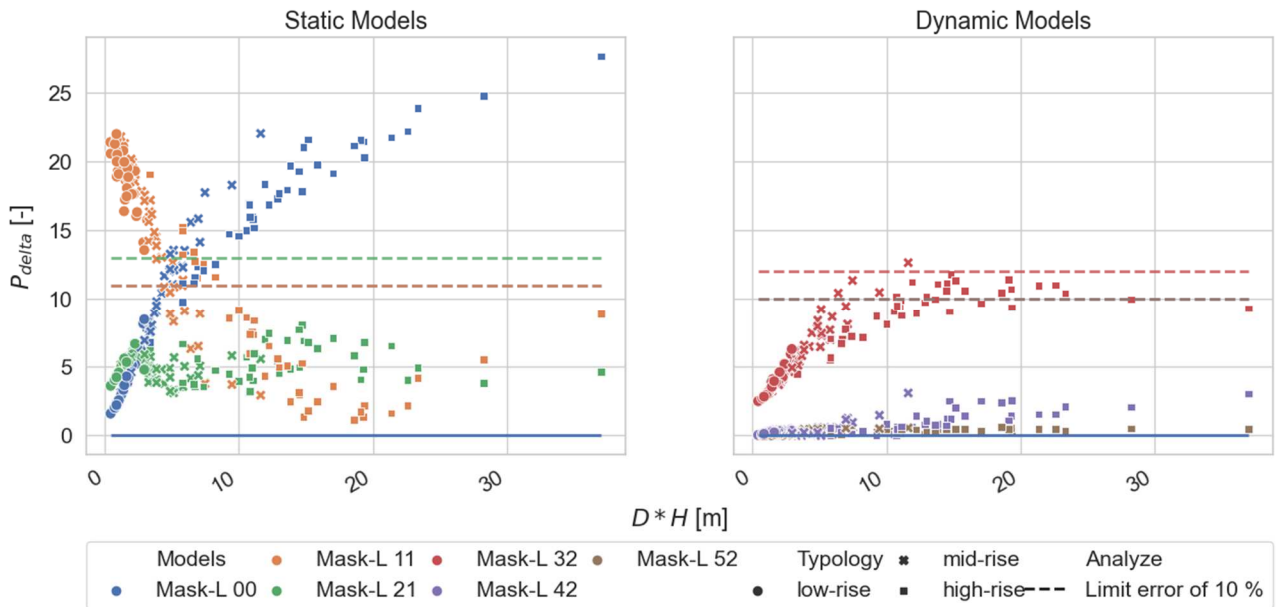
480 **3.2 Results for solar shading models**

481 As presented in [27], solar shading can strongly impact thermal dynamics as well as visual comfort or solar potential  
 482 ([46], [47]). In the study, the compared models are based on ray-tracing algorithm and static shading (3CL-DPE and  
 483 simple shading factors). The solar shading reference model is initially validated with DAYSIM [48]. Other  
 484 complementary studies on these models were performed on district size, weather and thermal building performance.  
 485 The seven solar models studied in [27] are summarised in Table 5.

486 *Table 5: Initial solar shading models*

Model <i>Software</i>	Characteristic	Representa tion
Mask-L 0.0	Without mutual shading	-
Mask-L 1.1	Constant annual factor of 0.5 on all buildings, mean value used when no mask model is implemented	-
Mask-L 2.1 <i>SMART-E</i>	Constant annual factor calculate for each building based on urban morphology	-
Mask-L 3.2 <i>DIMOSIM</i>	Dynamic calculation at the centre of each building	
Mask-L 4.2 <i>DIMOSIM</i>	Dynamic calculation at the centre of façade of each building	
Mask-L 5.2 <i>DIMOSIM</i>	Dynamic calculation at the centre of each building floors facade	
Mask-L 6.2 <i>DIMOSIM</i>	Dynamic calculation with simple mesh	

487 The same method is applied on the solar shading models, with a KGI composed of the density of the district (D) and the  
 488 mean height weighted by the building ground floor area (H). Figure 7 and Table 6 present the parsimony analysis  
 489 results for the thermal heating demand for districts with 36 buildings. As models do not differ much on the number of  
 490 parameters or simplifying hypothesis, the parsimony is never better than the reference model Mask-L 6.2. Only the  
 491 computation time for large districts and high buildings can advise to choose simpler solar shading models. The model  
 492 without shading (Mask-L 0.0) is only suitable for diffuse districts with small heights.



493

494

Figure 7: Parsimony criterion of district annual heating demand following the KGI DH – Solar shading models

495

Table 6: Models to prioritize for a district energy simulation following the DH for annual heating demand – Solar shading models

Modèles	DH [m]		
	<5	8	>12
Mask-L 6.2	Green	Green	Green
Mask-L 5.2	Yellow	Yellow	Yellow
Mask-L 4.2	Yellow	Yellow	Yellow
Mask-L 3.2	Yellow	Yellow with diagonal lines	Yellow
Mask-L 2.1	Yellow	Yellow with diagonal lines	Yellow
Mask-L 1.1	Red	Yellow with diagonal lines	Yellow
Mask-L 0.0	Yellow	Yellow with diagonal lines	Red

496

As the choice of solar shading models is very dependent on computation time because of the similar accuracy between

497

models and similar complexity, most of them are kept for the combination with zoning models. Only the Mask-L 1.1 is

498

put aside because of his arbitrary factor and poor results for low-rise districts. Even if the Mask-L 0.0 is the one with

499

the most parsimonious results, it is kept as it has been used for the zoning comparison and as it is still used in

500

several UBEM tools.

## 501 4 Comparison assessment of solar shading and thermal models with coupling

### 502 4.1 Selection of solar shading and thermal zoning models for coupling

503 Solar shading models become more and more detailed as the mesh of the sky vault and the walls become finer. This  
504 discretisation of walls is closely related to zoning as the solar gains vary according to geometry, altitude and  
505 orientation. The objective here is to see the impact on error when considering a more detailed zoning division.

506 The reference is taken as the combination of the two reference models: Mask-L 6.2 and *detailed floor* – EX – V. The  
507 *detailed floor* - EX shows very good parsimony results compared to the reference with a lower computation time. The  
508 model Mask-L 5.2 also presents few differences from the reference (Mask-L 6.2), with also lower computation time.  
509 Therefore, the models used for the combined reference are only used for it and are not combined with other models,  
510 reducing the number of model combinations. Table 7 summarises the zoning and solar shading models taken into  
511 account, with the models *detailed floor* – EX – V and Mask-L 6.2 only used as a reference combination. For  
512 simplification, abbreviations are used on the figures and when models are combined.

513 Table 7: Zoning and solar models selected for the combinations (EX: with conductive exchanges, V: with convective exchanges)

Zoning models		Solar shading models	
Model	Abbreviation	Model	Abbreviation
Detailed floor – EX – V	Reference	Mask-L 6.2	Reference
Detailed floor – EX	DF	Mask-L 5.2	M52
Detailed – EX	D	Mask-L 4.2	M42
Multiple floors – EX	MF	Mask-L 3.2	M32
3 floors – EX	3F	Mask-L 2.1	M21
Unique	U	Mask-L 0.0	M00

### 514 4.2 Simulation and districts specifications

515 Solar complementary studies allow to select districts morphologies on which the combination of zoning and solar  
516 models can be applied. In [27], 3 typologies of grid districts were taken from Bonhomme [49] (GENIUS project):

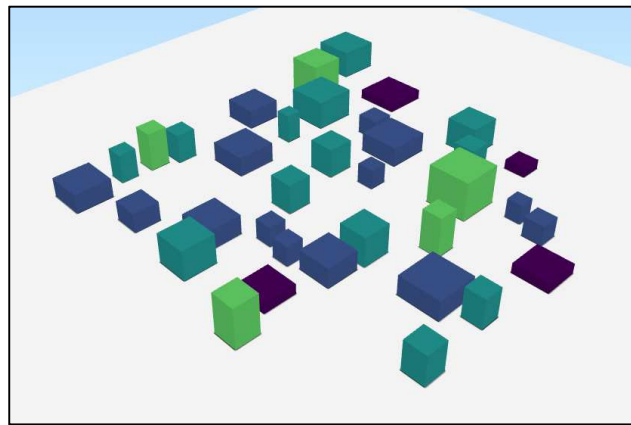
- 517 - *low-rise*: low buildings (3 – 20 m high) and sparse district (ground density from 0.05 to 0.38)
- 518 - *mid-rise*: mid-rise buildings (6 – 30 m high) with mid and high densities (ground density from 0.05 to 0.6)
- 519 - *high rise*: tall buildings (21 – 85 m high) and mid to high densities (ground density from 0.06 to 0.6)

520 3 districts from each typology are selected. For each, different district thermal performances are chosen:

- 521 - An old district with buildings before 1960 (single glazing windows, wall U-value between 1.6 and 3 W/m<sup>2</sup>.K  
522 and high infiltrations of 0.4)

- 523 - A common district with building between 1970-1990 with the first thermal regulations (single glazing  
524 windows, wall U-value between 0.4 and 2.4 W/m<sup>2</sup>.K and medium infiltrations of 0.2)
- 525 - A new district with buildings after 2006 (double glazing windows, wall U-value around 0.3 W/m<sup>2</sup>.K and very  
526 low infiltrations of 0.1)
- 527 - A mix district with 70% of new buildings and 30% of old buildings

528 Districts were randomly created with 16 and 36 buildings of different sizes and heights (i.e. 72 different districts). The  
529 buildings are randomly placed in the district until expected density is reached (Figure 8). Thermal characteristics are  
530 then set for each building, with a variation (max 10 %) from the initial value in order to have more diversity inside a  
531 district. As for the thermal zoning comparison, all systems and emitters are ideal and a one-year simulation with a 10  
532 min time step under Paris weather is used.



533

534 *Figure 8: Example of a low-rise random district*

### 535 **4.3 Results for simulation of models coupling**

#### 536 *4.3.1 Computation time*

537 Table 8 shows the different computation times for 2 mean districts of 16 buildings (the 6 meters high is the equivalent  
538 of a *low-rise* district and 39 m of a *high-rise* district). As for the application on a unique district, the use of simplified  
539 thermal zoning models highly accelerates the computation time, far more than the use of simplified solar shading  
540 models. However, these simplified solar shading models are useful for high districts, especially with the *detailed floor –*  
541 *EX* model. Indeed, using the simplest shading model Mask-L 0.0 reduces the computation time by more than one hour  
542 (with an acceleration factor of 1.5). The taller the building, the greater the number of thermal zones in the *detailed floor*  
543 *– EX* and *multiple floors – EX* models. The *multiple floors – EX* model shows a good speeding factor up to 11.4, but it

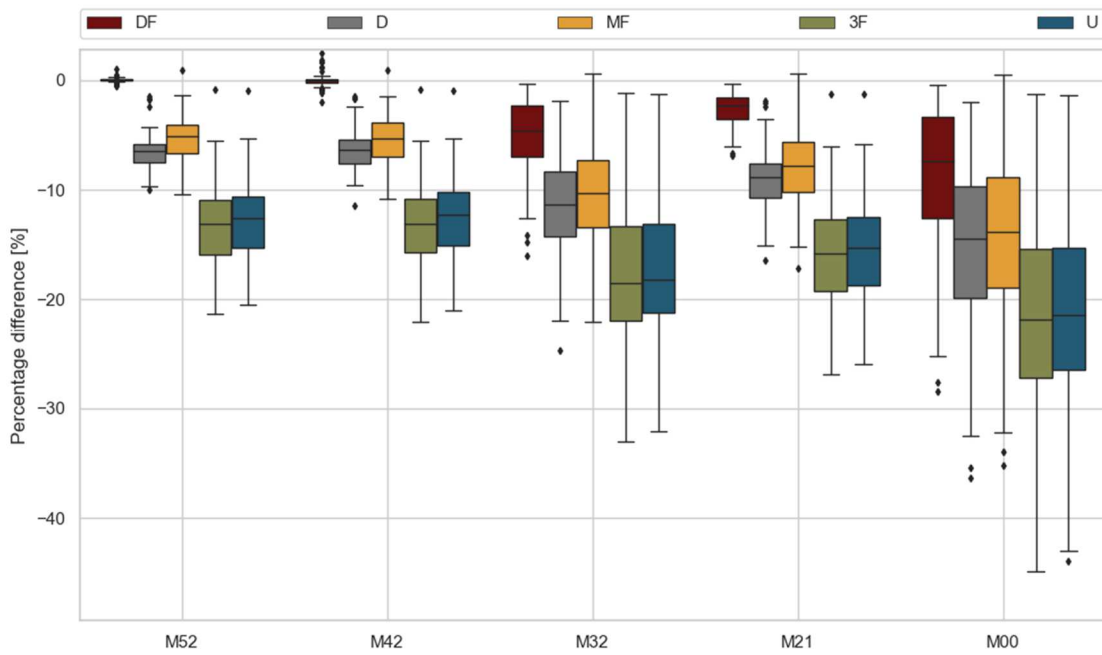
544 is more than 3 times lower than the other zoning models. When comparing differences between models for parsimony,  
 545 it is important to take into account computation time as there are many discrepancies between models.

546 *Table 8: Computation time for two districts of 16 buildings*

Zoning models	Solar models	H = 6m		H = 39m	
		t [s]	Speeding factor	t [s]	Speeding factor
<b>Reference</b>		910	1	15 810	1
DF	M52	940	1	16 160	1
	M42	940	1	15 010	1.1
	M32	930	1	12 040	1.3
	M21	950	1	11 040	1.4
	M00	920	1	10 730	1.5
D	M52	380	2.4	540	29.1
	M42	380	2.4	550	28.9
	M32	380	2.4	530	30
	M21	380	2.4	480	33.1
	M00	380	2.4	460	34.2
MF	M52	210	4.4	1400	11.3
	M42	210	4.4	1390	11.4
	M32	210	4.4	1450	10.9
	M21	200	4.5	1480	10.7
	M00	200	4.6	1430	11
3F	M52	180	5.1	310	50.9
	M42	170	5.2	280	55.8
	M32	170	5.3	250	63.7
	M21	170	5.3	240	66.1
	M00	170	5.5	240	65.9
U	M52	80	11.7	90	183.9
	M42	80	11.8	80	198.8
	M32	80	11.6	80	195.3
	M21	80	12	80	205.2
	M00	70	12.6	70	215.4

547 *4.3.2 Impact of models coupling on heating demand*

548 Figure 9 shows the differences between models according to thermal zoning and solar shading models. As in previous  
 549 simulations: the *detailed floor* – EX model shows accurate results; the *multiple floors* – EX and *detailed* – EX models  
 550 are close to each other; the *3 floors* – EX and *unique* models are also close, but with higher discrepancies.

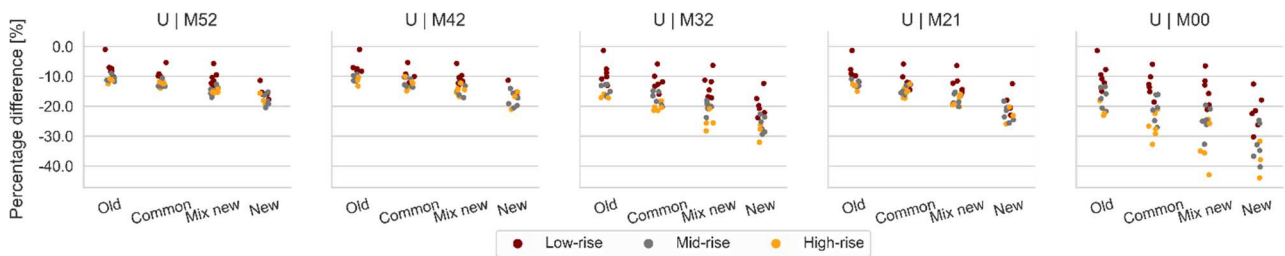


551

552 *Figure 9 : Annual thermal heating demand differences for the combination of solar shading and thermal zoning models on districts*

553 However, when simulating a whole district, solar shading between buildings impacts the results. The *detailed floor –*  
 554 *EX* model which was very close to the reference, shows differences up to 30 % if the solar shading is not modelled. The  
 555 errors increase quite homogeneously regardless of the thermal zoning model used. As in [27], the solar shading models  
 556 Mask-L 5.2 and 4.2 show close results. Although Mask-L 3.2 model has dynamic calculation, its results are not as good  
 557 as for Mask-L 2.1. At last, the Mask-L 0.0 model gives widely distributed results, with differences from less than 1 %  
 558 to more than 45 %.

559 With all these results, it is necessary to look deeper in the origin of the differences. In particular, the more thermally  
 560 efficient the district is (*mix new, new*), the greater the discrepancies. Figure 10 illustrates this trend with the *unique*  
 561 zoning model. In addition, differences increase with the height and density of the district: *low-rise* districts show  
 562 smaller differences than *high-rise* districts.



563

564 *Figure 10: Annual thermal heating demand differences for the combination of the Mask-L 0.0 model and thermal zoning models*

565

*following the thermal performance of districts*

566 4.3.3 Parsimony analysis of heating demand modelling

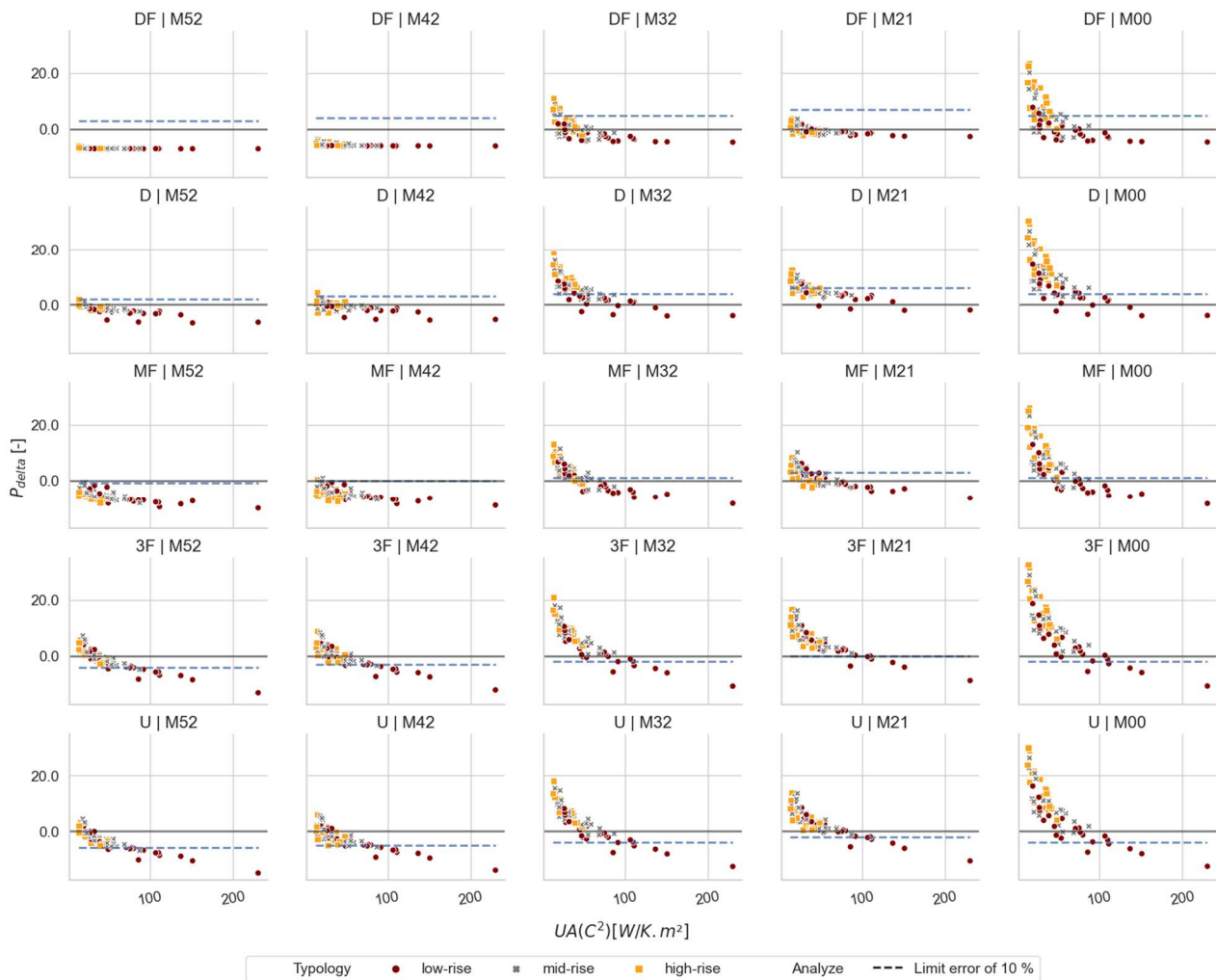
567 The objective is to find a KGI that takes into account the thermal and the morphological characteristics of districts. As  
568 in the thermal zoning study, Spearman coefficients are calculated giving (as expected) the same sensible parameters as  
569 previously, with the addition of the height and density from the solar shading models. Several combinations of  
570 parameters were tested to elaborate a KGI close to the previous one, with a stronger impact of the compactness (link to  
571 the morphology of buildings and so to the shading):

$$KGI_{final} = U_{bat} * A_{ground\ floor} * Compactness^2 = UAC^2 [W/K.m^2] \quad Eq. 11$$

572 The density could be taken into account in the KGI, but it only improves the parsimony trends for couple of models. As  
573 not all models behave the same according to one KGI,  $KGI_{final}$  is finally considered as the most balanced one for all  
574 models.

575 The Figure 11 presents the parsimony criterion for the annual heating demand according to the  $KGI_{final}$  and district  
576 typology. As before, the accuracy limit is set at 10 % (dotted line), the parsimony of the reference is 0 (solid line) and  
577 the weight factors of the criterion as 1. Table 9 is the transcription of the figure in a simpler way to help the user.

578 Low values of  $UAC^2$  represent *high-rise* districts with good thermal performance. For these types of districts, the choice  
579 of models is restricted to detailed ones, as *3 floors – EX* and *unique* models are not accurate enough. But as the  $UAC^2$   
580 increases, the use of simple models becomes legitimate, even the simplest combination U – M00 for a  $UAC^2$  greater  
581 than 150 W/K.m<sup>2</sup>. However, the thermal zoning model that could almost be used regardless of the KGI and solar model  
582 is the *detailed floor – EX* model.



583

584

Figure 11: Parsimony criterion  $P_{delta}$  for annual heating demand following the  $UAC^2$  - 16 and 36 buildings per district

585

586

587

588

589

The parsimony criterion values for the *3 floors* – EX and *unique* models are similar, with only a slight difference for the Mask-L 2.1 solar shading model. However, all the simulated buildings have only one usage, so the influence of floor division is reduced. Therefore, as the *3 floors* – EX model is 4 times faster than the *multiple floors* – EX model, *3 floors* – EX could make a good compromise between the models *unique* and *multiple floors* – EX when several usages in the building must be modelled.

590

591

592

593

Contrary to the previous results, the *detailed* – EX zoning model shows a good parsimony when used with detailed solar models: by taking into account the inter-effects between buildings, thermal zoning division per orientation shows a good accuracy with a better solar gains distribution. Nevertheless, the *multiple floors* – EX model still presents better results than this model, in particular with simpler solar models.

594 Solar models differ from each other especially through the solar calculation mesh used to determine the shading factors.  
 595 The Mask-L 5.2 and 4.2 have similar results, with slight differences for low KGI value. The static solar shading model  
 596 Mask-L 2.1 shows for all zoning models better results than the dynamic model Mask-L 3.2.

597 *Table 9: Models to prioritize for a district energy simulation following the UAC<sup>2</sup> for annual heating demand - 16 and 36 buildings*  
 598 *per district*

Zoning models	Solar models	UAC <sup>2</sup> [W/K.m <sup>2</sup> ]														
		25	50	60	80	90	100	120	130	150	190	200	220	320		
Reference	Reference															
DF	M52	Green	Green	Green	Green	Green	Green	Green	Green	Green	Green	Green	Green	Green	Green	Green
DF	M42	Green	Green	Green	Green	Green	Green	Green	Green	Green	Green	Green	Green	Green	Green	Green
DF	M32	Orange	Orange	Yellow	Yellow	Green										
DF	M21	Yellow	Yellow	Yellow	Yellow	Green										
DF	M00	Red	Red	Red	Red	Yellow	Yellow	Yellow	Green							
D	M52	Yellow	Yellow	Green												
D	M42	Red	Yellow	Yellow	Green											
D	M32	Red	Red	Red	Red	Red	Red	Yellow								
D	M21	Red	Red	Red	Red	Yellow										
D	M00	Red	Red	Red	Red	Red	Red	Red	Red	Red	Red	Red	Red	Red	Red	Red
MF	M52	Green	Green	Green	Green	Green	Green	Green	Green	Green	Green	Green	Green	Green	Green	Green
MF	M42	Red	Red	Red	Red	Red	Red	Red	Red	Red	Red	Red	Red	Red	Red	Red
MF	M32	Red	Red	Red	Red	Red	Red	Red	Red	Red	Red	Red	Red	Red	Red	Red
MF	M21	Red	Red	Yellow												
MF	M00	Red	Red	Red	Red	Red	Red	Red	Red	Red	Red	Red	Red	Red	Red	Red
3F	M52	Red	Red	Red	Red	Red	Red	Red	Red	Red	Red	Red	Red	Red	Red	Red
3F	M42	Red	Red	Red	Red	Red	Red	Red	Red	Red	Red	Red	Red	Red	Red	Red
3F	M32	Red	Red	Red	Red	Red	Red	Red	Red	Red	Red	Red	Red	Red	Red	Red
3F	M21	Red	Red	Red	Red	Red	Red	Red	Red	Red	Red	Red	Red	Red	Red	Red
3F	M00	Red	Red	Red	Red	Red	Red	Red	Red	Red	Red	Red	Red	Red	Red	Red
U	M52	Red	Red	Red	Red	Red	Red	Red	Red	Red	Red	Red	Red	Red	Red	Red
U	M42	Red	Red	Red	Red	Red	Red	Red	Red	Red	Red	Red	Red	Red	Red	Red
U	M32	Red	Red	Red	Red	Red	Red	Red	Red	Red	Red	Red	Red	Red	Red	Red
U	M21	Red	Red	Red	Red	Red	Red	Red	Red	Red	Red	Red	Red	Red	Red	Red
U	M00	Red	Red	Red	Red	Red	Red	Red	Red	Red	Red	Red	Red	Red	Red	Red

599 Finally, the most parsimonious models are the DF – M52 for low UAC<sup>2</sup>, then the MF – M52 and at the end the U –  
 600 M52. The solar shading model Mask-L 4.2 is not the most parsimonious one, but gives good results and could be used  
 601 for *high-rise* districts to speed up the simulation (see Table 8). Indeed, the computation time can be restrictive for the  
 602 use of the DF – M52 model and may then lead the user to choose simpler models. Thus, the choice of models must be  
 603 adapted to the district in order to have a parsimonious modelling as well as an acceptable computation time.

## 604 **5 Discussion**

605 While the issue of thermal zoning design has already been closely studied at building scale, few studies address this  
606 issue at urban scale, and even less with the problematic of solar shading calculation. Nevertheless, the two types of  
607 models are strongly linked since zones distribution and shaded solar gains influence the overheating distribution. The  
608 present study is therefore contributing to the analysis of the impact of such inter-effect and to the assessment of the  
609 complexity and accuracy of such coupling.

610 This study has shown that the use of very detailed models gives in some cases worse results than simpler models,  
611 especially when the thermal exchanges between zones are not modelled. This illustrates the importance of global  
612 consistency when choosing and coupling thermal models. Furthermore, the lack of data at district level implies the  
613 simplification of the inter-zone ventilation model. This simplification certainly does not model these exchanges  
614 properly, especially when interior design is almost neglected. The extension of the initial simulation to various climates  
615 also shows how difficult it can be to give a single answer to the question: “what is the good combination of models, and  
616 how the diversity of the urban characteristics influences the parsimony?”. In the future, other urban contexts should be  
617 studied to extend this analysis.

618 Indeed, the diversity of simulations objectives, districts and models is difficult to manage. Here, only the KPI “thermal  
619 heating demand” has been studied on specific buildings and districts. The methodology has been applied on other KPIs,  
620 showing differences in the determination of KGIs and the choice of models. Moreover, the considered buildings are  
621 only composed of dedicated profiles and uses that are similar. Other variants have to be studied to take into account the  
622 diversity of occupation and uses in districts. Other building geometries or zoning designs must then be developed. Even  
623 if the aim of using virtual districts was to create realistic diversity, the methodology should be tested on real districts.

624 The study is here only comparative without any validation as the gathering of energy consumption data at district scale  
625 is too complex nowadays. This introduces a bias because the reference is taken as the most detailed model. Moreover,  
626 the parameters are considered valid, simply taking into account the complexity of the data recovery as a disadvantage.  
627 Therefore, data determination in an uncertain context should be also undertaken.

628 This paper contributes to the discussion on the complexity of models and on the issues of how and when to choose  
629 them, especially here for thermal zoning design and solar shading calculation. A simple decision colour table has been  
630 produced to guide the modellers and users and help them understand the complexity of urban building energy

631 simulation. It can also be used as a decision support depending on the stage of a project, finding a good trade-off  
632 between required accuracy, time allowed for the project stage and available data.

## 633 **6 Conclusion**

634 This paper proposes a methodology to apprehend parsimonious modelling of urban scale energy simulation. This  
635 methodology first identifies different modelling families to compare them independently. Then it determines a  
636 simulation design plan to simulate virtual districts (created to generate diversity) with the chosen models. The results  
637 are then used to calculate a parsimony criterion, which is used in conjunction with *key guidance indicators* (KGI).  
638 These KGIs help to detect the most parsimonious models for a given output according to district characteristics. *These*  
639 *KGIs have been built on macro parameters of the district to guide the user. A first sensibility analysis with Spearman*  
640 *coefficients allows to reduce the number of parameters to consider. Then, knowledge from building expert is used to*  
641 *combine them. A further methodology has to be constructed to identify these KGIs in a more systematic way. In order*  
642 *to apprehend parsimony at urban scale, a definition of parsimony is proposed as a trade-off between the number of*  
643 *parameters, the number of simplifying hypothesis, the accuracy of the model and the computation time for a given*  
644 *simulation objective. A parsimony criterion is created based on the first three characteristics, leaving the time cost to*  
645 *the subjective choice of the user, as the computing power at user disposal can be too variable. The methodology has*  
646 *been demonstrated on the UBEM DIMOSIM in this article. It would be interesting to apply it to other tools in order to*  
647 *confirm its reproducibility and the use of identical KGIs. Furthermore, this methodology must be then combined to data*  
648 *uncertainty in the context of urban simulation in order to have a more complete analysis of UBEM models: on data and*  
649 *on models.*

650 This methodology is first applied on thermal zoning models coupled with conductive and convective exchanges models  
651 for the simulation of annual heating demand. Several independent buildings are simulated with all the models  
652 combinations. From the simulated buildings, entire districts are randomly created to create a representative diversity of  
653 the French building stock. The parsimony criterion is applied on each district for all the selected models, and a limit of  
654 accuracy of 10 % compared to the reference is taken. A KGI is created, namely UAC<sup>2</sup>, based on compactness, thermal  
655 performance and buildings area. The lower the KGI, the greater the differences. This comparison led to the  
656 determination of two main parsimonious models, both simulated with conductive exchanges: *detailed floor* and *multiple*  
657 *floors*. The simplest thermal zoning models are only relevant for high values of KGI, without being the most  
658 parsimonious ones. When taking the computation time into account, *detailed floor* models show a high computational

659 cost, encouraging the use of the *multiple floors* model. [These conclusions must be confirmed by further tests on real](#)  
660 [cases with more complex building geometries.](#)

661 Thermal zoning design is strongly related to solar radiation, as the discretisation of facades can influence the calculation  
662 of shading factors due to urban morphology. Therefore, a subset of the previous models is selected to be coupled with  
663 several solar shading models and applied to virtual districts with different heights, densities and thermal performances.  
664 The same methodology is applied on these model combinations and a new KGI is created to take into account the  
665 district morphology impact. The results show that the choice of model combination varies strongly according to the  
666 morphology and the thermal performance of district. Three different parsimonious models following the KGI value are  
667 identified: *detailed floor* with conductive exchanges, *multiple floors* with conductive exchanges and *unique*, all coupled  
668 with solar shading model Mask-L 5.2. However, considering the computation time, the *detailed floor* model could be  
669 replaced by another parsimonious model giving sufficient accuracy to speed up the simulation.

670 This study shows the impact of thermal zoning designs, but also their relative influence with solar shading. This  
671 highlights the importance of considering solar shading models at district scale. Understanding these impacts and the  
672 idea of parsimony could lead to more balanced and consistent district simulations, which need to be specifically adapted  
673 to the case study.

## 674 **7 Acknowledgments**

675 This research did not receive any specific grant from funding agencies in the public, commercial, or not-for-profit  
676 sectors.

677

- 679 [1] International Energy Agency, Ed., *Transition to sustainable buildings: strategies and opportunities to 2050*.  
680 Paris: IEA Publ, 2013.
- 681 [2] United Nations, ‘World Urbanization Prospects - The 2018 Revision’, United Nations, Department of Economic  
682 and Social Affairs, Population Division, New York, ST/ESA/SER.A/366, 2018. [Online]. Available:  
683 <https://population.un.org/wup/Publications/>.
- 684 [3] P. Riederer, V. Partenay, N. Perez, C. Nocito, R. Trigance, and T. Guiot, ‘Development Of A Simulation  
685 Platform For The Evaluation Of District Energy System Performances’, in *Proceedings of BS2015: 14th  
686 Conference of International Building Performance Simulation Association*, Hyderabad, India, 2015, pp. 2499–  
687 2506.
- 688 [4] T. Berthou, B. Duplessis, P. Rivière, P. Stabat, D. Casetta, and D. Marchio, ‘SMART-E: A Tool For Energy  
689 Demand Simulation And Optimization At The City Scale’, in *Proceedings of BS2015: 14th Conference of IBPSA*,  
690 Hyderabad, India, Dec. 2015, pp. 1782–1789.
- 691 [5] J. Fonseca, T.-A. Nguyen, A. Schlueter, and F. Maréchal, ‘City Energy Analyst (CEA): Integrated framework for  
692 analysis and optimization of building energy systems in neighborhoods and city districts’, *Energy Build.*, vol.  
693 113, Dec. 2015, doi: 10.1016/j.enbuild.2015.11.055.
- 694 [6] D. Robinson *et al.*, ‘CITYSIM: Comprehensive Micro-Simulation of Resource Flows For Sustainable Urban  
695 Planning’, in *Proceedings of BS2009: 11th Conference of International Building Performance Simulation  
696 Association*, Glasgow, Scotland, 2009, pp. 1083–1090.
- 697 [7] Y. Chen, T. Hong, and M. A. Piette, ‘Automatic generation and simulation of urban building energy models  
698 based on city datasets for city-scale building retrofit analysis’, *Appl. Energy*, vol. 205, pp. 323–335, Nov. 2017,  
699 doi: 10.1016/j.apenergy.2017.07.128.
- 700 [8] Y. Heo, R. Choudhary, and G. A. Augenbroe, ‘Calibration of building energy models for retrofit analysis under  
701 uncertainty’, *Energy Build.*, vol. 47, pp. 550–560, Apr. 2012, doi: 10.1016/j.enbuild.2011.12.029.
- 702 [9] A. Vandermeulen, B. van der Heijde, and L. Helsen, ‘Controlling district heating and cooling networks to unlock  
703 flexibility: A review’, *Energy*, vol. 151, pp. 103–115, May 2018, doi: 10.1016/j.energy.2018.03.034.
- 704 [10] S. Troitzsch *et al.*, ‘Optimal electric-distribution-grid planning considering the demand-side flexibility of thermal  
705 building systems for a test case in Singapore’, *Appl. Energy*, vol. 273, p. 114917, Sep. 2020, doi:  
706 10.1016/j.apenergy.2020.114917.
- 707 [11] L. Kurdgelashvili, J. Li, C.-H. Shih, and B. Attia, ‘Estimating technical potential for rooftop photovoltaics in  
708 California, Arizona and New Jersey’, *Renew. Energy*, vol. 95, pp. 286–302, Sep. 2016, doi:  
709 10.1016/j.renene.2016.03.105.
- 710 [12] M. Bagheri, N. Shirzadi, E. Bazdar, and C. A. Kennedy, ‘Optimal planning of hybrid renewable energy  
711 infrastructure for urban sustainability: Green Vancouver’, *Renew. Sustain. Energy Rev.*, vol. 95, pp. 254–264,  
712 Nov. 2018, doi: 10.1016/j.rser.2018.07.037.
- 713 [13] C. Klemm and P. Vennemann, ‘Modeling and optimization of multi-energy systems in mixed-use districts: A  
714 review of existing methods and approaches’, *Renew. Sustain. Energy Rev.*, vol. 135, p. 110206, Jan. 2021, doi:  
715 10.1016/j.rser.2020.110206.
- 716 [14] N. Perez, P. Riederer, and C. Inard, ‘Development of a multiobjective optimization procedure dedicated to the  
717 design of district energy concept’, *Energy Build.*, vol. 178, pp. 11–25, Nov. 2018, doi:  
718 10.1016/j.enbuild.2018.07.061.
- 719 [15] N. Perez, P. Riederer, C. Inard, and V. Partenay, ‘Thermal Building Modelling Adapted To District Energy  
720 Simulation’, in *Proceedings of BS2015: 14th Conference of International Building Performance Simulation  
721 Association*, Hyderabad, India, Dec. 2015, pp. 270–277, doi: 10.13140/RG.2.1.3714.2163/1.
- 722 [16] L. Frayssinet, F. Kuznik, J.-L. Hubert, M. Milliez, and J.-J. Roux, ‘Adaptation of building envelope models for  
723 energy simulation at district scale’, *Energy Procedia*, vol. 122, pp. 307–312, Sep. 2017, doi:  
724 10.1016/j.egypro.2017.07.327.
- 725 [17] L. Frayssinet *et al.*, ‘Simulating the energy loads at the district scale: Introduction to a dedicated platform’, in  
726 *Proceedings of BS2019: 16th Conference of International Building Performance Simulation Association*, Rome,  
727 Italy, 2019, vol. Proceedings of Building Simulation 2019, pp. 1467–1474, doi:  
728 10.26868/25222708.2019.210819.
- 729 [18] Y. Han, J. E. Taylor, and A. L. Pisello, ‘Exploring mutual shading and mutual reflection inter-building effects on  
730 building energy performance’, *Appl. Energy*, vol. 185, pp. 1556–1564, Jan. 2017, doi:  
731 10.1016/j.apenergy.2015.10.170.
- 732 [19] D. Robinson and A. Stone, ‘Solar radiation modelling in the urban context’, *Sol. Energy*, vol. 77, no. 3, pp. 295–  
733 309, Sep. 2004, doi: 10.1016/j.solener.2004.05.010.

- 734 [20] R. Compagnon, 'RADIANCE: a simulation tool for daylighting systems'. LESO-PB, EPFL, 2001.
- 735 [21] Y. Chen and T. Hong, 'Impacts of building geometry modeling methods on the simulation results of urban  
736 building energy models', *Appl. Energy*, vol. 215, pp. 717–735, Apr. 2018, doi: 10.1016/j.apenergy.2018.02.073.
- 737 [22] S. Sun and J.-L. Bertrand-Krajewski, 'Sélection d'un modèle hydrologique conceptuel parcimonieux pour  
738 différents objectifs', *NOVATECH*, p. 5, 2013.
- 739 [23] M. N. Karim, C. M. Reid, L. Tran, A. Cochrane, and B. Billah, 'Variable selection methods for multiple  
740 regressions influence the parsimony of risk prediction models for cardiac surgery', *J. Thorac. Cardiovasc. Surg.*,  
741 vol. 153, no. 5, pp. 1128–1135.e3, May 2017, doi: 10.1016/j.jtcvs.2016.11.028.
- 742 [24] M. W. Alldredge, K. H. Pollock, T. R. Simons, and S. A. Shriner, 'Multiple-species analysis of point count data:  
743 a more parsimonious modelling framework', *J. Appl. Ecol.*, vol. 44, no. 2, pp. 281–290, 2007, doi:  
744 10.1111/j.1365-2664.2006.01271.x.
- 745 [25] H. Akaike, 'A new look at the statistical model identification', *IEEE Trans. Autom. Control*, vol. 19, pp. 716–  
746 722, 1974.
- 747 [26] D. Posada and T. Buckley, 'Model Selection and Model Averaging in Phylogenetics: Advantages of Akaike  
748 Information Criterion and Bayesian Approaches Over Likelihood Ratio Tests', *Syst. Biol.*, vol. 53, pp. 793–808,  
749 Nov. 2004, doi: 10.1080/10635150490522304.
- 750 [27] E. Garreau, T. Berthou, B. Duplessis, V. Partenay, and D. Marchio, 'Urban-scale Energy Simulation: A  
751 Development Of A Novel Method For Parsimonious Modelling - The Example Of Solar Shading Model  
752 Calculation', in *Proceedings of Building Simulation 2019: 16th Conference of IBPSA*, Rome, Italy, 2019, pp.  
753 3258–3265, doi: 10.26868/25222708.2019.210344.
- 754 [28] M. Heidarinejad *et al.*, 'Demonstration of reduced-order urban scale building energy models', *Energy Build.*, vol.  
755 156, pp. 17–28, Dec. 2017, doi: 10.1016/j.enbuild.2017.08.086.
- 756 [29] CEREMA, 'Table des Fichiers Fonciers', 2018. [http://piece-jointe-carto.developpement-  
757 durable.gouv.fr/NAT004/DTerNP/html3/\\_ff\\_descriptif\\_tables\\_liste.html](http://piece-jointe-carto.developpement-durable.gouv.fr/NAT004/DTerNP/html3/_ff_descriptif_tables_liste.html) (accessed Nov. 08, 2019).
- 758 [30] M. Bonhomme, H. Ait Haddou, and L. Adolphe, 'GENIUS: A tool for classifying and modelling evolution of  
759 urban typologies', presented at the 28th Conference, Opportunities, Limits & Needs Towards an environmentally  
760 responsible architecture, Lima, Peru, Jan. 2012, [Online]. Available: <https://hal.insa-toulouse.fr/hal-02157256>.
- 761 [31] Intelligence Energy Europe Programme, 'TABULA - Bâtiments résidentiels Typologie du parc existant et  
762 solutions exemplaires pour la rénovation énergétique en France', European Union, 2015. [Online]. Available:  
763 <http://episcopo.eu/communication/download/>.
- 764 [32] Programme PACTE, 'RAGE, Analyse détaillée du parc résidentiel existant. (Detailed analysis of the existing  
765 residential building stock)', Ministère de la cohésion des territoires et des relations avec les collectivités  
766 territoriales, rev 2017 2012. [Online]. Available: [http://www.programmepacte.fr/analyse-detaillee-du-parc-  
767 residentiel-existant-rapport](http://www.programmepacte.fr/analyse-detaillee-du-parc-residentiel-existant-rapport).
- 768 [33] A. Saltelli *et al.*, *Global Sensitivity Analysis. The Primer*. Chichester, UK: John Wiley & Sons, Ltd, 2007.
- 769 [34] M. Martin, N. H. Wong, D. J. C. Hii, and M. Ignatius, 'Comparison between simplified and detailed EnergyPlus  
770 models coupled with an urban canopy model', *Energy Build.*, vol. 157, pp. 116–125, Dec. 2017, doi:  
771 10.1016/j.enbuild.2017.01.078.
- 772 [35] L. Rivalin, D. Marchio, P. Stabat, M. Caciolo, and B. Cogné, 'Influence of building zoning on annual energy  
773 demand', presented at the 3rd International High Performance Buildings Conference, Purdue, USA, 2014.
- 774 [36] Y. Heo, G. Ren, and M. Sunikka-Blank, 'Investigating an Adequate Level of Modelling for Energy Analysis of  
775 Domestic Buildings', presented at the 3rd Asia conference of International Building Performance Simulation  
776 Association - ASim2016, Mar. 2018, doi: 10.17863/CAM.21153.
- 777 [37] L. Smith, 'Beyond the Shoebox: Thermal Zoning Approaches for Complex Building Shapes', *ASHRAE Trans.*,  
778 vol. 118, p. 8, 2012.
- 779 [38] Autodesk, *Autodesk Revit*. Autodesk.
- 780 [39] M. Shin and J. S. Haberl, 'Thermal zoning for building HVAC design and energy simulation: A literature  
781 review', *Energy Build.*, vol. 203, p. 109429, Nov. 2019, doi: 10.1016/j.enbuild.2019.109429.
- 782 [40] T. Dogan, C. Reinhart, and P. Michalatos, 'Autozoner: An algorithm for automatic thermal zoning of buildings  
783 with unknown interior space definitions', *J. Build. Perform. Simul.*, pp. 1–14, Feb. 2015, doi:  
784 10.1080/19401493.2015.1006527.
- 785 [41] T. Dogan and C. Reinhart, 'Shooboxer: An algorithm for abstracted rapid multi-zone urban building energy  
786 model generation and simulation', *Energy Build.*, vol. 140, pp. 140–153, Apr. 2017, doi:  
787 10.1016/j.enbuild.2017.01.030.
- 788 [42] G.-E. Kyriakodis, P. Riederer, and E. Bozonnet, 'Towards the development of a coupled model for district  
789 simulation: buildings, energy systems and microclimate co-simulation', in *IBPSA France 2018*, Bordeaux,  
790 France, May 2018, vol. hal-02005502.
- 791 [43] ENVI\_MET GmbH, *Envi-MET Software*. ENVI\_MET GmbH.
- 792 [44] DesignBuilder Software Ltd, *DesignBuilder*. DesignBuilder Software Ltd.

- 793 [45] M. Caciolo, 'Analyse expérimentale et simulation de la ventilation naturelle mono-façade pour le  
794 rafraîchissement des immeubles de bureaux', PhD thesis, École Nationale Supérieure des Mines de Paris, 2010.
- 795 [46] A. L. Pisello, J. E. Taylor, X. Xu, and F. Cotana, 'Inter-building effect: Simulating the impact of a network of  
796 buildings on the accuracy of building energy performance predictions', *Build. Environ.*, vol. 58, pp. 37–45, Dec.  
797 2012, doi: 10.1016/j.buildenv.2012.06.017.
- 798 [47] L. Romero Rodríguez, R. Nouvel, E. Duminil, and U. Eicker, 'Setting intelligent city tiling strategies for urban  
799 shading simulations', *Sol. Energy*, vol. 157, pp. 880–894, Nov. 2017, doi: 10.1016/j.solener.2017.09.017.
- 800 [48] C. Reinhart and P.-F. Breton, 'Experimental validation of 3DS MAX design 2009 and DAYSIM 3.0', in  
801 *Proceedings of BS2011: 12th Conference of International Building Performance Simulation Association*,  
802 Glasgow, Scotland, Jul. 2009, pp. 1514–1521, doi: 10.1582/LEUKOS.2009.06.01001.
- 803 [49] M. Bonhomme, 'Contribution à la génération de bases de données multi-scalaires et évolutives pour une  
804 approche pluridisciplinaire de l'énergétique urbaine', Université de Toulouse, 2013.
- 805

# GRAPHICAL ABSTRACT

No graphical abstract is proposed.